Monatshefte für Chemie 117, 557—572 (1986)

Monatshefte für Chemie
Chemical Monthly

The Influence of Additives on the X-Ray Induced Aggregation of Malate Synthase
Monitoring of the Aggregation Process *in situ* by Time-Resolved Small-Angle X-Ray Scattering

Peter Zipper[a,*], **Manfred Kriechbaum**[a], **Rudolf Wilfing**[a], and **Helmut Durchschlag**[b]

[a] Institut für Physikalische Chemie, Universität Graz, A-8010 Graz. Austria
[b] Institut für Biophysik und Physikalische Biochemie, Universität Regensburg, D-8400 Regensburg, Federal Republic of Germany

(Received 23 April 1985. Revised 30 September 1985. Accepted 20 November 1985)

The X-ray induced aggregation of the sulfhydryl enzyme malate synthase in aqueous solution was monitored *in situ* by time-resolved small-angle X-ray scattering. Experiments were performed in the absence/presence of various additives: formate, superoxide dismutase, catalase, NaCl, acetyl-CoA, glyoxylate, malate, pyruvate, α-ketobutyrate, oxaloacetate, glycollate, lactate. The scattering curves were measured as a function of the time of irradiation and were analysed in terms of radii of gyration, degrees of aggregation, distance distribution functions, and parameters derived therefrom. Irradiation in the absence of additives resulted in a strong aggregation of enzyme particles. Each of the additives impeded aggregation, however to a different extent. The $OH^{\cdot}$ scavenger formate reduced aggregation efficiently; less pronounced effects were registered for superoxide dismutase and/or catalase (the scavengers for $O_2^{\cdot-}$ and H_2O_2), and for NaCl. Very pronounced diminutions of the aggregation phenomena were provided by substrates or analogues; the efficiency of these substances as radioprotectors may be explained by their action as both scavengers and specific ligands. Based on these results some implications for the performance of conventional small-angle X-ray scattering experiments on biopolymers are derived.

(Keywords: Additives; Aggregation; Malate synthase; Radiation damage; Radioprotection; Time-resolved small-angle X-ray scattering)

Der Einfluß von Zusätzen auf die röntgeninduzierte Aggregation der Malatsynthase. Registrierung des Aggregationsvorganges in situ mittels zeitaufgelöster Röntgenkleinwinkelstreuung

Die röntgeninduzierte Aggregation des Sulfhydrylenzyms Malatsynthase in wäßriger Lösung wurde *in situ* mittels zeitaufgelöster Röntgenkleinwinkel-

streuung messend verfolgt. Streuexperimente wurden in An- bzw. Abwesenheit verschiedener Zusätze durchgeführt: Formiat, Superoxiddismutase, Catalase, NaCl, Acetyl-CoA, Glyoxylat, Malat, Pyruvat, α-Ketobutyrat, Oxalacetat, Glycolat, Lactat. Die Streukurven wurden als Funktion der Bestrahlungsdauer registriert. Die Auswertung lieferte Streumassenradien, Aggregationsgrade, Abstandsverteilungsfunktionen, und daraus abgeleitete Parameter. Die Bestrahlung in Abwesenheit von Zusätzen verursachte eine starke Aggregation der Enzymteilchen. Jeder der Zusätze verminderte die Aggregation, wenn auch in unterschiedlichem Ausmaß. Der $OH^{\cdot}$ Fänger Formiat verringerte die Aggregation wirksam; weniger stark ausgeprägte Effekte ergaben sich für die $O_2^{\cdot-}$ bzw. H_2O_2 Fänger Superoxiddismutase bzw. Catalase und für NaCl. Substrate und Substratanaloge reduzierten das Ausmaß der Aggregation besonders wirkungsvoll; der Schutzeffekt dieser Substanzen kann durch ihre zweifache Wirkung als Fänger bzw. spezifische Liganden erklärt werden. Ausgehend von diesen Ergebnissen werden einige Schlußfolgerungen für die Durchführung üblicher Röntgenkleinwinkelexperimente an Biopolymeren abgeleitet.

Introduction

Small-angle X-ray scattering (SAXS) is a very powerful method for studying the structure of biopolymers in solution [1–3]. Under certain conditions biopolymers may suffer radiation damages during SAXS experiments, e.g. aggregation phenomena in the case of sulfhydryl proteins, especially in dilute buffers [4–8]. While such phenomena may be a serious handicap in conventional SAXS studies, the SAXS method may be used, on the other hand, successfully to monitor the damage process *in situ;* the latter approach has been introduced by us as a novel technique in the field of radiation biology [4–11]. Our investigations have been performed with several proteins, particularly with the sulfhydryl enzyme malate synthase.

Malate synthase catalyses the condensation of glyoxylate and acetyl-CoA to form malate and CoA. Several substrate analogues, like pyruvate, oxaloacetate, α-ketobutyrate, glycollate were shown to bind to the enzyme and to inhibit the enzyme for glyoxylate, while lactate did not show comparable effects [12–16]. The enzyme from baker's yeast has a molecular weight of about 185 000 (presumably 3 subunits); it is of oblate shape and undergoes slight conformational changes upon ligand binding (acetyl-CoA, glyoxylate, pyruvate) [4, 16–20].

Monitoring of the X-ray induced aggregation of malate synthase *in situ* by time-resolved SAXS has established the aggregation to proceed in one and later on in two dimensions; several substances, such as dithiothreitol (*DTT*), ethanol, the substrates acetyl-CoA and glyoxylate, and the substrate analogue pyruvate were found to impede aggregation [4, 5, 7, 8, 21, 22]. Mainly $OH^{\cdot}$ radicals, but also $O_2^{\cdot-}$ and H_2O_2, were held responsible for the X-ray damage of the enzyme in aqueous air-saturated

solution [5, 8, 22]. In order to differentiate between the effects caused by these deleterious species, we investigated the radiation damage of malate synthase in the absence/presence of specific scavengers: formate as a scavenger for $OH^{\cdot}$, superoxide dismutase (*SOD*) for $O_2^{\cdot-}$ and catalase for H_2O_2. Inactivation and repair experiments and SAXS investigations on pre-irradiated samples of malate synthase established distinct protective effects of the mentioned scavengers [23–25].

In this paper we report on time-resolved SAXS experiments which monitored the X-ray induced aggregation of malate synthase in the absence/presence of various additives, including both scavengers and substrates or analogues. Our investigations were aimed (i) to get further insight into the role of the various kinds of additives in protecting the enzyme against radiation damage, and (ii) to elucidate the efficiency of additives as possible radioprotectors in conventional SAXS experiments. A preliminary report has already been presented [26].

Materials and Methods

Malate synthase (EC 4.1.3.2) was isolated from baker's yeast in electrophoretically pure form [16]. Catalase (EC 1.11.1.6) from bovine liver, superoxide dismutase (*SOD*; EC 1.15.1.1) from bovine erythrocytes, and acetyl-CoA were obtained from Boehringer, Mannheim. Sodium formate, glyoxylic acid, and NaCl were purchased from Merck, Darmstadt; sodium pyruvate and sodium lactate from Serva, Heidelberg; oxaloacetic acid and sodium malate from Roth, Karlsruhe; sodium α-ketobutyrate and glycolic acid from Sigma, Munich. All other reagents were of A-grade purity. Quartz-bidistilled water was used throughout.

Solutions: A 5 m*M* Tris/HCl buffer *pH* 8.1, containing 10 m*M* $MgCl_2$, 1 m*M* MgK_2*EDTA*, 0.2 m*M DTT*, was used as a standard buffer. Malate synthase was dialysed against this buffer. For experiments, carefully prepared stock solutions of malate synthase and additives (all *pH* 8.1) were mixed to give the final concentrations of samples listed in Table 1.

Small-Angle X-Ray Scattering: SAXS experiments were performed by means of *Kratky* cameras as in previous studies [5, 7], with two different enzyme preparations under similar experimental conditions. The unfiltered radiation from a Philips PW 2253/11 X-ray tube (Cu, 50 kV, 30 mA) served as primary radiation. All samples were investigated at 4 °C in *Mark* capillaries of about 1 mm diameter. The effective integral primary intensity P_0 (i.e. the flux of CuK_α and K_β quanta per cm of beam length after transmitting the sample) amounted to $6.7–7.4 \cdot 10^7$ counts $s^{-1}\,cm^{-1}$, as determined by means of a calibrated Lupolen platelet [27]. Additionally the power absorbed by the samples was determined as about 1.4 μW by means of a *Fricke* dosimeter. Each scattering curve was measured repeatedly in the angular range $2.6 \leqslant 2\theta \leqslant 62$ mrad; one measuring cycle took about 4–5 h. Experiments were extended up to irradiation times of 60 h. Usually the scattering curves were interpreted without any desmearing; in some selected cases correction for slit-length smearing was performed analytically [28]. Distance distribution functions $p(r)$ were calculated from the desmeared scattering curves, applying conventional *Fourier* transformation.

Results

For each sample (cf. Table 1) scattering curves were recorded at definite time intervals while the sample was exposed permanently to the primary radiation. *Guinier* plots of the innermost portion of slit-smeared scattering curves of 4 representative samples are shown in Fig. 1. These plots clearly demonstrate that the scattering behaviour of malate synthase depends on the time of irradiation and the nature and concentration of additives: the curves obtained in the absence of additives (sample 1) reflect a very pronounced aggregation phenomenon; the presence of additives obviously impedes aggregation (9 or 90 m*M* formate: samples 5 and 9) or suppresses aggregation completely (90 m*M* malate: sample 21).

The *Guinier* plots of all 21 samples were analysed for the apparent mean radius of gyration, $\tilde{R}$, and the slit-smeared intensity at zero angle, $\tilde{I}(0)$, as a function of the time t of X-irradiation in the SAXS camera. The ratio of the zero intensities $\tilde{I}(0)$ at time t and at $t = 0$ yielded the apparent

Table 1. *Composition of samples 1–21 used for the SAXS experiments with malate synthase*[a]

Sample Number	Additives
1	none
2	0.3 μM *SOD*
3	50 nM catalase
4	0.3 μM *SOD* + 50 n*M* catalase
5	9 m*M* formate
6	9 m*M* formate + 0.3 μ*M SOD*
7	9 m*M* formate + 50 n*M* catalase
8	9 m*M* formate + 0.3 μ*M SOD* + 50 n*M* catalase
9	90 m*M* formate
10	90 m*M* formate + 0.3 μ*M SOD*
11	90 m*M* formate + 50 n*M* catalase
12	90 m*M* formate + 0.3 μ*M SOD* + 50 n*M* catalase
13	90 m*M* NaCl
14	4 m*M* acetyl-CoA
15	90 m*M* glyoxylate
16	90 m*M* pyruvate
17	90 m*M* α-ketobutyrate
18	90 m*M* oxaloacetate
19	90 m*M* glycollate
20	90 m*M* lactate
21	90 m*M* malate

[a] Final concentration of malate synthase: $\approx 55\,\mu M$ (≈ 10 mg/ml).

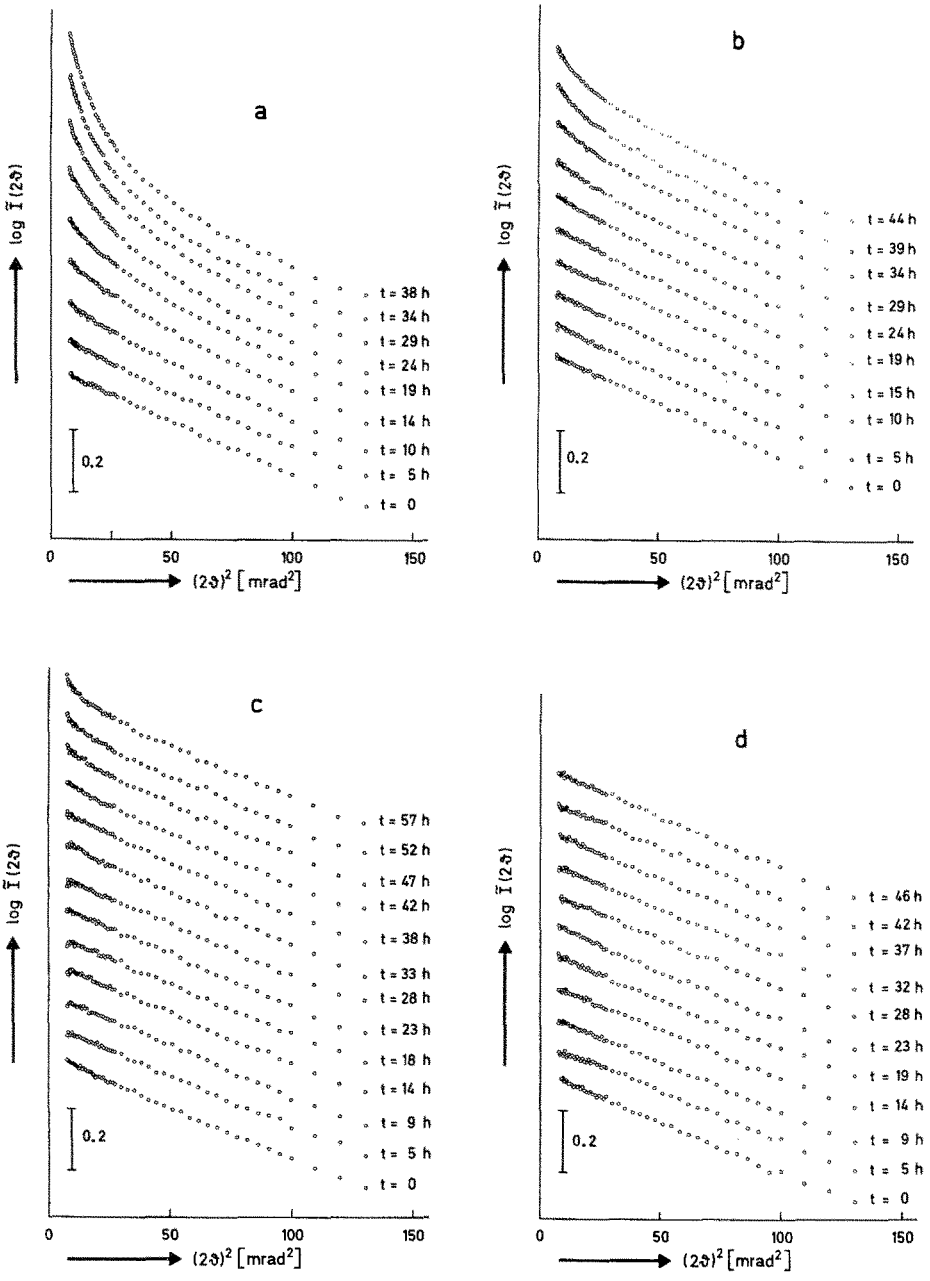

Fig. 1. *Guinier* plots of experimental slit-smeared scattering curves of some selected samples as a function of time t of X-irradiation in the SAXS camera. For convenience the curves are shifted by multiples of 0.1 logarithmic units on the ordinate. a: sample 1; b: sample 5; c: sample 9; d: sample 21. Composition of samples cf. Tab. 1

mean degree of aggregation, $\tilde{x}$. The corresponding values for $\tilde{R}$ and $\tilde{x}$ of samples 1, 5, 9, 21 are listed in Table 2.

Fig. 2 presents the distance distribution functions $p(r)$ of samples 1, 5, 9, 21, obtained from *Fourier* transforms of the desmeared scattering curves. According to the theory [2, 5], the $p(r)$ functions are measures for the frequency of distances within a particle, and equal zero for all distances larger than the maximum particle diameter. The curves in Fig. 2 convincingly show the increase in particle size (aggregation) as a function of time and additive.

Mean radii of gyration, $\bar{R}$, and mean degrees of aggregation, $\bar{x}$, of samples 1, 5, 9, 21, as derived from the desmeared scattering curves or from the $p(r)$ functions, are also listed in Table 2. Differences between the true parameters ($\bar{R}$, $\bar{x}$) and the corresponding apparent quantities ($\tilde{R}$, $\tilde{x}$) increase with progressing aggregation; this is in accord with the theory of desmearing.

As has been shown previously [4–7], the radiation induced changes of the radius of gyration and the degree of aggregation can be presented in so-called stability plots. These plots may be derived from both apparent and true quantities, leading to equivalent conclusions concerning the aggregation behaviour of irradiated samples. We prefer the stability plots derived from the apparent quantities in order to avoid possible errors introduced during the desmearing procedure. Therefore, as in the previous studies, the data were plotted as $(\tilde{R}/\tilde{R}_1)^2$ vs. t^2 and $\tilde{x}$ vs. t^2, where $\tilde{R}/\tilde{R}_1$ is the ratio of the apparent radii of gyration at time t and at $t=0$. Fig. 3 presents such stability plots for 14 selected samples: each curve characterizes the aggregation behaviour of malate synthase in the presence of another additive; all curves show a linear course, either from the very

Table 2. *Aggregation of malate synthase upon X-irradiation in the SAXS camera in the presence of selected additives*

Sample Number	t[a] (h)	$\tilde{R}$[b] (nm)	$\tilde{x}$[c]	$\bar{R}$[d,f] (nm)	$\bar{x}$[e,f]
1	0	3.7	1.00	3.9	1.00
	4.8	4.1	1.04	4.5	1.11
	9.6	4.5	1.10	5.5	1.33
	14.4	5.0	1.22	6.2	1.60
	19.2	6.0	1.39	7.9	2.25
	24.0	7.1	1.68	9.2	3.3
	28.8	8.2	2.04	11.1	5.0
	33.5	9.6	2.55	12.5	7.5
	38.3	10.8	3.1	13.8	10.5

Table 2 (continued)

Sample Number	t[a] (h)	$\tilde{R}$[b] (nm)	$\tilde{x}$[c]	$\bar{R}$[d,f] (nm)	$\bar{x}$[e,f]
5	0	3.8	1.00	3.9	1.00
	4.8	3.9	1.01	4.0	1.02
	9.7	3.9	1.01	4.1	1.02
	14.5	4.0	1.02	4.0	1.04
	19.3	4.1	1.04	4.6	1.12
	24.1	4.4	1.07	5.1	1.20
	29.0	4.8	1.12	6.2	1.39
	33.8	5.6	1.23	7.9	1.77
	38.7	6.5	1.35	9.7	2.38
	43.5	7.4	1.49	—	—
9	0	3.7	1.00	3.8	1.00
	4.6	3.7	1.00	—	—
	9.1	3.7	1.00	3.9	1.01
	13.7	3.7	1.01	3.9	1.02
	18.3	3.7	0.99	3.9	0.99
	22.8	3.7	0.99	3.9	1.01
	27.7	3.7	0.98	4.0	1.00
	32.6	4.4	1.06	—	—
	37.5	3.9	1.02	4.2	1.07
	42.4	4.4	1.04	5.8	1.21
	47.3	5.0	1.09	7.2	1.40
	52.1	5.7	1.14	9.3	1.77
	57.0	6.4	1.23	—	—
21	0	3.7	1.00	3.9	1.00
	4.6	3.7	1.01	—	—
	9.3	3.7	0.98	3.9	0.98
	13.9	3.6	0.98	3.8	0.97
	18.5	3.7	1.00	3.9	0.99
	23.1	3.9	1.00	—	—
	27.8	3.6	0.98	3.8	0.97
	32.4	3.7	0.98	3.8	0.96
	37.0	3.8	0.99	3.9	0.97
	41.7	3.7	0.98	3.9	0.99
	46.3	3.7	0.99	—	—

[a] Time of irradiation in the SAXS camera.

[b] Apparent mean radius of gyration, determined from the slit-smeared intensities $\tilde{I}(2\theta)$.

[c] Apparent mean degree of aggregation, $\tilde{x} = \tilde{I}(0)_t/\tilde{I}(0)_{t=0}$.

[d] Mean radius of gyration, determined from the desmeared intensities $I(2\theta)$ or from the distance distribution function $p(r)$.

[e] Mean degree of aggregation, determined from $I(0)_t/I(0)_{t=0}$ or from the distance distribution function $p(r)$.

[f] For technical reasons the desmearing procedure could not be performed in all cases.

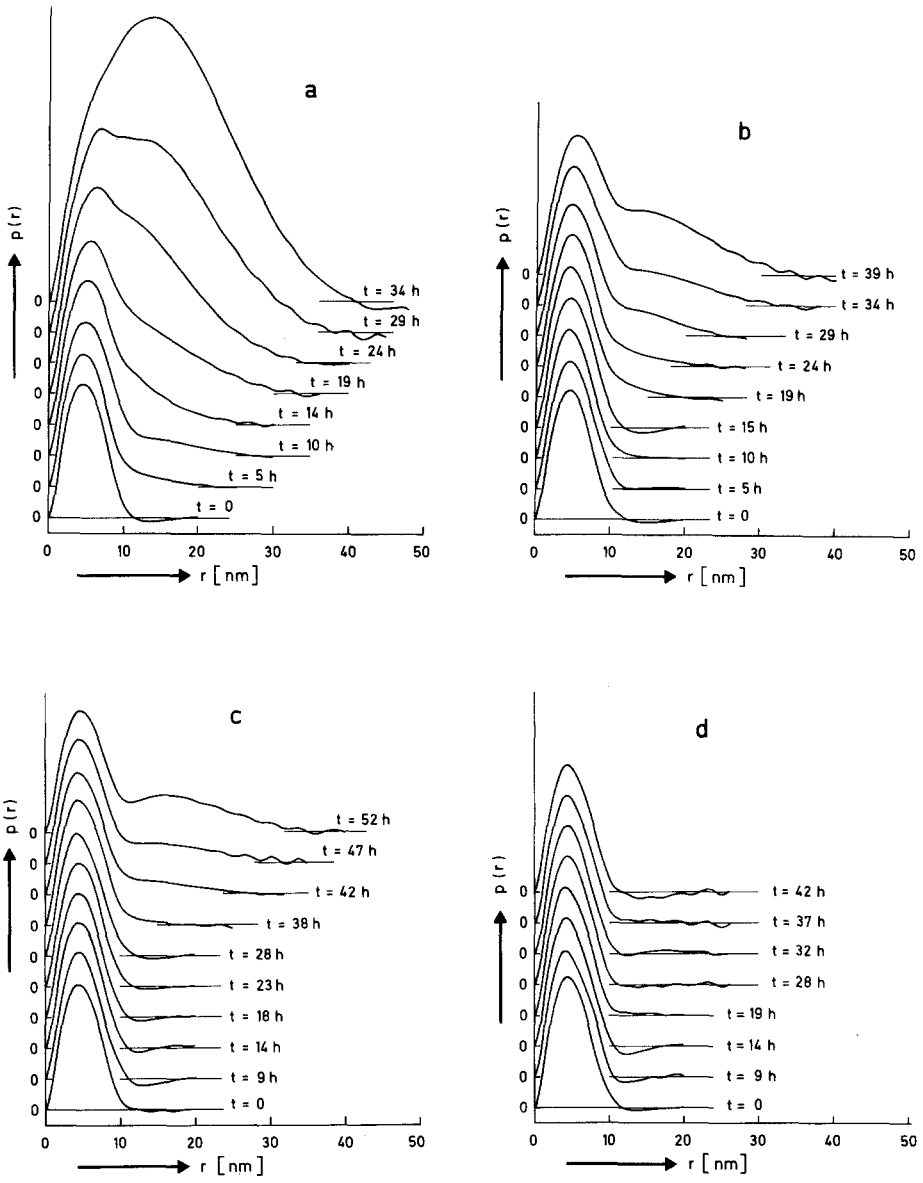

Fig. 2. Distance distribution functions $p(r)$ of samples 1, 5, 9, 21 (cf. Fig. 1) as a function of time t of X-irradiation in the SAXS camera. For clear presentation the $p(r)$ functions have been smoothed slightly to reduce disturbing oscillations

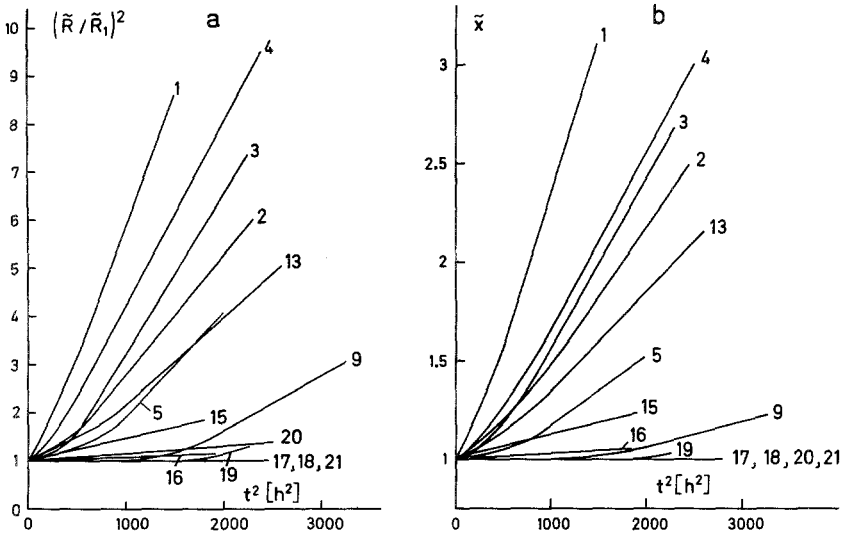

Fig. 3. Stability plots showing the dependence of the apparent mean radius of gyration, $\tilde{R}$, and of the apparent mean degree of aggregation, $\tilde{x}$, of malate synthase on the time t of X-irradiation in the SAXS camera in the presence of various selected additives. $\tilde{R}_1$ is the apparent radius of gyration of the unaggregated enzyme ($t = 0$). The numbering of curves follows the designations of samples given in Tab. 1

beginning or, after a lag-phase, at higher t^2 values. It has been established in our previous work [4–7] that the slopes of the linear ranges in such plots may be used as a measure for the rate of enzyme aggregation. The rate constants, $k_{\tilde{R}}^2 = \mathrm{d}(\tilde{R}/\tilde{R}_1)^2/\mathrm{d}(t^2)$ and $k_{\tilde{x}}^2 = \mathrm{d}\,\tilde{x}/\mathrm{d}(t^2)$, of all 21 samples are given in Table 3. Fig. 3 and Table 3 convincingly demonstrate that each of the additives is able to reduce the rate of aggregation of malate synthase.

Discussion and Conclusions

Protective Effects of Additives Against Aggregation

Though all additives used in this study may act as radioprotectors against X-ray induced aggregation of malate synthase, the efficiency of the various additives, however, is clearly different. It ranges from a rather weak protection, as provided by *SOD* or catalase, to a virtually complete protection, as provided e.g. by malate, oxaloacetate, or α-ketobutyrate. In interpreting the different magnitude of protective effects one has to take into account that the enzymes *SOD* and catalase were only present in catalytic concentrations, in contrast to all other additives.

Table 3. *Rate constants, $k_{\tilde{R}}^2$ and $k_{\tilde{x}}^2$, for X-ray induced structural changes of malate synthase in the presence of additives*

Sample Number	Enzyme[a]	$P_0 \cdot 10^{-7}$[b] (counts s^{-1} cm^{-1})	$k_{\tilde{R}}^2 \cdot 10^5$[c] ($h^{-2}$)	$k_{\tilde{x}}^2 \cdot 10^5$[d] ($h^{-2}$)
1	I	6.78	550	160
	II	6.79	510	160
2	I	6.90	250	71
3	I	6.99	330	87
4	I	6.89	380	90
	II	6.76	390	120
5	II	6.71	220	35
6	II	6.80	160	29
7	II	6.83	150	25
8	II	6.72	160	31
9	I	6.92	110	13
	II	7.09	160	21
10	II	7.38	120	19
11	II	7.26	89	11
12	II	7.32	110	19
13	I	6.69	180	51
14	I	6.92	12	0
15	I	6.90	50	8.2
16	I	6.90	7.6	3.4
17	I	6.85	0	0
18	I	6.89	0	0
19	I	6.85	0[e]	0[e]
20	I	6.85	15	0
21	I	6.79	0	0

[a] Experiments were performed with two different enzyme preparations (I, II) under similar conditions.

[b] Effective integral primary intensity (CuK_α plus K_β quanta).

[c] Slopes $d(\tilde{R}/\tilde{R}_1)^2/d(t^2)$, determined from the ascending linear branches of the curves in stability plots $(\tilde{R}/\tilde{R}_1)^2$ vs. t^2 (cf. Fig. 3 a).

[d] Slopes $d\tilde{x}/d(t^2)$, determined from the ascending linear branches of the curves in stability plots $\tilde{x}$ vs. t^2 (cf. Fig. 3 b).

[e] Value refers to the lag-phase.

The protective effects provided by the specific scavengers (formate, *SOD*, and catalase) confirm the involvement of $OH^{\cdot}$, $O_2^{\cdot-}$, and H_2O_2 in the aggregation of X-irradiated malate synthase. Similar conclusions have been drawn previously from SAXS investigations on pre-irradiated samples [25]. It is obvious that the protective effect of formate depends on the concentration of this additive, and may be slightly modified by the simultaneous presence of *SOD* and/or catalase.

The protective effect observed for NaCl may be ascribed partly to the scavenging of $OH^{\cdot}$ by Cl^{-} (cf. [29]). Screening of the enzyme particles by electrostatic interactions and unspecific binding of the salt may also be taken into consideration. The latter argument, of course, also holds for the other additives when present in high concentrations.

The effect of the substrate acetyl-CoA is superior to that of the substrate glyoxylate, in accord with previous findings [5, 7]. The product of the enzyme reaction, malate, shows an even more pronounced protective effect. Also the substrate analogues (pyruvate, α-ketobutyrate, oxaloacetate, glycollate) are able to protect the enzyme with high efficiency; the same is true for lactate.

Among all substrates and analogues investigated, the substrate glyoxylate impedes the aggregation least. In this context it should be mentioned, however, that glyoxylate is a very effective protector against X-ray induced inactivation of malate synthase, where it is clearly superior to pyruvate [5, 8, 30]. Malate protects the enzyme against inactivation to a similar extent as glyoxylate [30].

It is plausible that the protective efficiency of the substrates and analogues is partially due to their scavenging capability (e.g. pyruvate: $k_{OH^{\cdot}} = 3.2 \cdot 10^7\, M^{-1}\, s^{-1}$ at $pH\,9$, [31]). But the comparison of the different behaviour of glyoxylate, malate, and pyruvate in aggregation and inactivation, and the comparison of these substances with the typical $OH^{\cdot}$ scavenger formate ($k_{OH^{\cdot}} = 2.4 \cdot 10^9\, M^{-1}\, s^{-1}$ at $pH\,9$, [32]) suggest that part of the protective effects of the substrates and analogues is due to their specific binding to the enzyme. When considering the effect of lactate, it should be mentioned that this additive may not only act as a potent scavenger ($k_{OH^{\cdot}} = 4.8 \cdot 10^9\, M^{-1}\, s^{-1}$ at $pH\,9$, [32]) but may also be oxidized as a consequence of X-irradiation to give pyruvate [33], which then may also act as a specific ligand.

With some samples the aggregation phenomena became manifest only after a considerable lag-phase (cf. Fig. 3: e.g. samples 9 and 19). Possible explanations for this behaviour may include consumption of the additive, consumption of oxygen, formation of noxious secondary products from the additive.

A comparison of present and previous [5] kinetic data in a plot of $\log k_R^2$ vs. P_0 is given in Fig. 4. The primary intensity P_0 may be taken as a measure for the absorbed X-ray dose rate. While the values at 0.2 or 2 mM *DTT* show a distinct dependence of $\log k_R^2$ on P_0, the results in the presence of glyoxylate, pyruvate, or acetyl-CoA behave in a different manner. It has to be clarified by future experiments whether this different behaviour is due to different mechanisms of protection (scavenging, specific ligand binding).

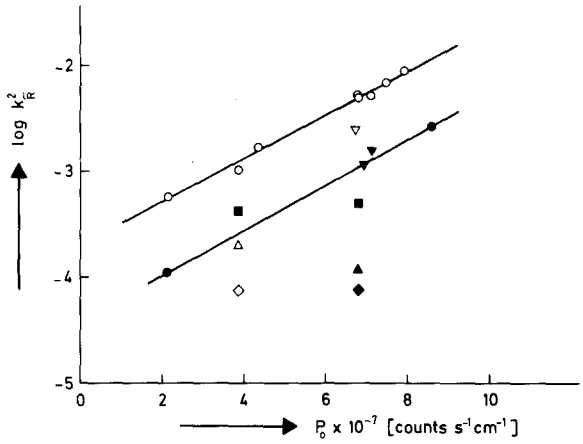

Fig. 4. Dependence of rate constants, k_R^2, on integral primary intensity, P_0, and nature and concentration of additives, as obtained in this and previous papers [5, 7]. ○: 0.2 m*M DTT;* ●: 2 m*M DTT*; ▽: 9 m*M* formate; ▼: 90 m*M* formate; ■: 90 m*M* glyoxylate; △: 2 m*M* acetyl-CoA; ▲: 4 m*M* acetyl-CoA; ◇: 50 m*M* pyruvate; ◆: 90 m*M* pyruvate

Shape Factors

In the case of a monodisperse system of aggregates of radius of gyration R, composed of x identical particles of radius of gyration R_1, the ratio $(R/R_1)^2/x$ depends on the shape of the aggregates (cf. [21]) and may be called "shape factor". With a polydisperse system of aggregates the analogous ratio $(\bar{R}/R_1)^2/\bar{x}$ is a function of both the shape of aggregates and their molecular weight distribution. Fig. 5 shows plots of $\tilde{f} = (\tilde{R}/\tilde{R}_1)^2/\tilde{x}$ vs. $\tilde{x}$ and $\bar{f} = (\bar{R}/R_1)^2/\bar{x}$ vs. $\bar{x}$ for three representative samples (0, 9, 90 m*M* formate: samples 1, 5, 9). Irrespective of the use of apparent or true quantities, similar patterns are obtained. At a given mean degree of aggregation the shape factors, $\tilde{f}$ and $\bar{f}$, increase with the concentration of formate. This indicates that the diminution of aggregation by the $OH^{\cdot}$ scavenger formate is accompanied by a change of the size distribution of aggregates, whereby the percentage of large aggregates is increased. A similar behaviour as found in the absence of formate (sample 1) is observed in the presence of *SOD* or catalase or NaCl (samples 2, 3, 4, 13; not shown in Fig. 5).

Comparison Between in situ Irradiated and Pre-irradiated Samples

Recent SAXS experiments [25] on samples of malate synthase pre-irradiated in the absence or presence of formate yielded mean radii of

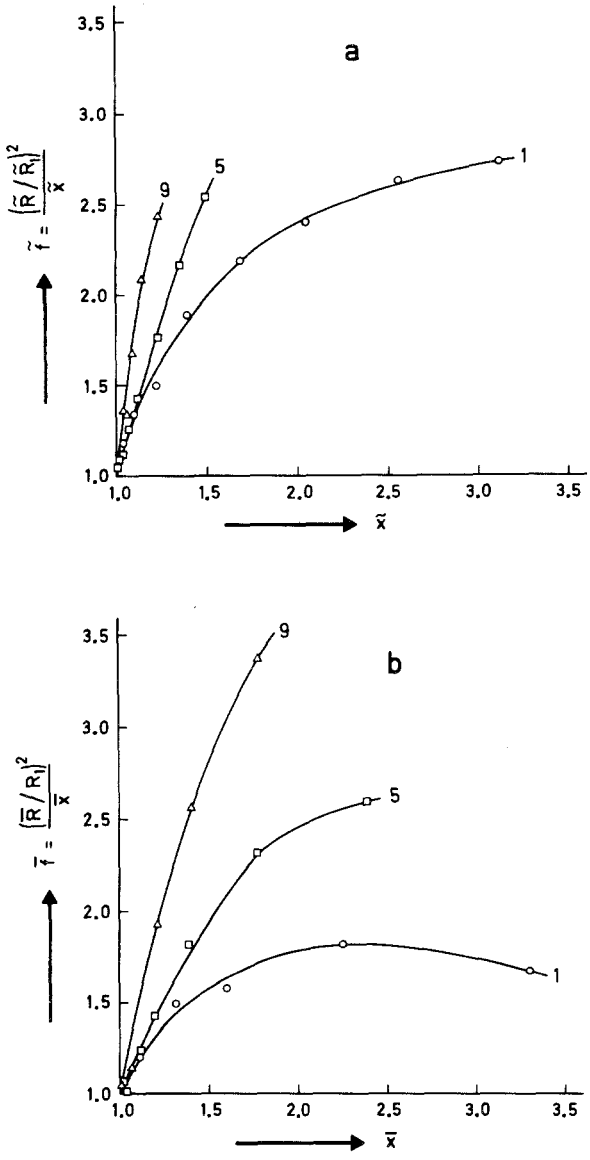

Fig. 5. Shape factors $\tilde{f}$ and $\bar{f}$ of malate synthase X-irradiated in the absence or presence of formate (samples 1, 5, 9) as a function of $\tilde{x}$ or $\bar{x}$

Table 4. *Mean radii of gyration, $\bar{R}$, and mean degrees of aggregation, $\bar{x}$, of malate synthase pre-irradiated with 6 kGy in the absence or presence of formate*[a]

Additive	$\bar{R}$ (nm)	$\bar{x}$
none	13.3	5.7
10 m*M* formate	9.1	1.6
100 m*M* formate	6.5	1.2

[a] Data selected from Ref. [25].

gyration and mean degrees of aggregation (cf. Table 4), which may be compared with our present data with respect to $\bar{R}$ and $\bar{x}$ (cf. Table 2). The comparison reveals that in the absence of formate or at low formate concentration an irradiation for about 30 h in the SAXS camera leads to similar $\bar{x}$ values as the pre-irradiation of samples with 6 kGy; at the high formate concentration an irradiation time of about 40 h is necessary to produce a comparable $\bar{x}$. Comparable $\bar{R}$ values are achieved after slightly longer irradiation times.

While for the pre-irradiation of samples the entire volume was X-irradiated [5, 25], in the SAXS camera only a thin zone of the capillary ($0.2 \times 1 \times 35\,mm^3$, cf. Fig. 6) is directly hit by the primary beam. In order

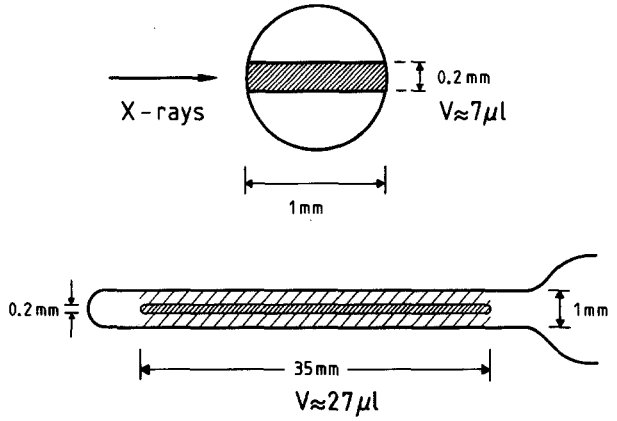

Fig. 6. Schematic drawing of the geometry of the *Mark* capillary used in the SAXS camera. Above: cross-section; below: longitudinal section, not according to scale. The zone hit directly by the primary beam ($V \simeq 7\,\mu l$) is densely hatched on the drawing

to decide whether the energy absorbed in this zone is restricted to this small volume (7 μl) or will be dissipated over a larger volume (e.g. by diffusion of radiolysis products of water), we may proceed in the following way: If we divide the mentioned 6 kGy by 30 h we obtain formally a dose rate of 200 Gy h^{-1}, corresponding to 56 mGy s^{-1}. When the absorbed power of 1.4 μW (cf. Materials and Methods) is divided by this dose rate, we obtain a mass of 25 mg, corresponding to a volume of 25 μl. This implies that in the absence of formate the absorbed energy is dissipated over a volume given by the cross-section of the capillary and the beam length ($V \simeq 27\,\mu$l; cf. Fig. 6). At high formate concentration, the corresponding calculation leads to a larger volume of 34 μl. This reflects the conversion of $OH^{\cdot}$ radicals to less reactive products which may diffuse over larger distances.

Implications for Conventional SAXS Investigations

Though our present results for malate synthase in the given buffer cannot be transferred quantitatively to other systems, some conclusions may be drawn for the performance of conventional SAXS experiments on biopolymers. The presence of catalytic amounts of *SOD* or catalase (0.01 mg/ml) or of small amounts of $OH^{\cdot}$ scavengers (e.g. $\geqslant 10$ m*M* formate) or of salt (e.g. $\geqslant 100$ m*M* NaCl) may reduce unwanted X-ray induced aggregation phenomena considerably. In the light of these considerations use of too dilute buffers (< 100 m*M*) should be avoided because buffer components may also act as scavengers. Compounds like *DTT* or *EDTA*, which are frequent constituents of buffers, may reduce radiation damages of biopolymers additionally [5, 6, 8, 18, 22].

Acknowledgements

We wish to express gratitude to Prof. Dr. *J. Schurz*, Graz, and to Prof. Dr. *R. Jaenicke*, Regensburg, for their interest in the problem. Skilful assistance by Mrs. *S. Richter* in preparing solutions is gratefully acknowledged. *P. Z.* is much obliged to the Austrian Academy of Sciences for the supply of X-ray devices; *H. D.* thanks the Deutsche Forschungsgemeinschaft for support.

References

[1] *Pilz I, Glatter O, Kratky O*, Methods enzymol (1979) Academic Press, New York-London, vol 61 p 148
[2] *Glatter O, Kratky O* (eds) (1982) Small angle X-ray scattering. Academic Press, London-New York
[3] *Kratky O* (1983) Nova acta leopoldina. Neue Folge 55: 1
[4] *Zipper P, Durchschlag H* (1977) Biochem Biophys Res Commun 75: 394
[5] *Zipper P, Durchschlag H* (1980) Radiat Environ Biophys 18: 99

[6] *Zipper P, Gatterer HG, Schurz J, Durchschlag H* (1980) Monatsh Chem 111: 981
[7] *Zipper P, Durchschlag H* (1980) Monatsh Chem 111: 1367
[8] *Zipper P, Durchschlag H* (1981) Monatsh Chem 112: 1
[9] *Zipper P, Durchschlag H* (1978) Abstr 12th FEBS-Meeting, Dresden 1978, Abstr No 2545
[10] *Zipper P, Durchschlag H* (1980) Abstr 5th Int Conf on Small-Angle Scattering, Berlin 1980, p 230
[11] *Zipper P, Durchschlag H, Gatterer HG* (1983) Proc 7th Int Congr Radiat Res, Amsterdam 1983, No A 5–15, Martinus Nijhoff Publ, Amsterdam
[12] *Wong DTO, Ajl SJ* (1956) J Amer Chem Soc 78: 3230
[13] *Dixon GH, Kornberg HL, Lund P* (1960) Biochim Biophys Acta 41: 217
[14] *Eggerer H, Klette A* (1967) Eur J Biochem 1: 447
[15] *Biedermann G* (1972) Thesis, University of Regensburg
[16] *Durchschlag H, Biedermann G, Eggerer H* (1981) Eur J Biochem 114: 255
[17] *Durchschlag H, Goldmann K, Wenzl S, Durchschlag G, Jaenicke R* (1977) FEBS Lett 73: 247
[18] *Zipper P, Durchschlag H* (1978) Eur J Biochem 87: 85
[19] *Zipper P, Durchschlag H* (1978) Z Naturforsch 33c: 504
[20] *Durchschlag H, Bogner F, Wilhelm D, Jaenicke R, Zipper P, Mayer F* (1978) Hoppe-Seyler's Z Physiol Chem 359: 1077
[21] *Zipper P, Durchschlag H* (1980) Z Naturforsch 35c: 890
[22] *Durchschlag H, Zipper P* (1981) Z Naturforsch 36c: 516
[23] *Durchschlag H, Zipper P* (1984) Biochem Biophys Res Commun 118: 364
[24] *Durchschlag H, Zipper P* (1985) Radiat Environ Biophys 24: 99
[25] *Zipper P, Wilfing R, Kriechbaum M, Durchschlag H* (1985) Z Naturforsch 40c: 364
[26] *Zipper P, Durchschlag H* (1983) Proc 7th Int Congr Radiat Res, Amsterdam 1983, No A 4–38, Martinus Nijhoff Publ, Amsterdam
[27] *Kratky O, Pilz I, Schmitz PJ* (1966) J Colloid Interface Sci 21: 24
[28] *Zipper P* (1972) Acta Phys Austriaca 36:27
[29] *Anbar M, Thomas JK* (1964) J Phys Chem 68: 3829
[30] *Durchschlag H, Zipper P,* manuscript in preparation
[31] *Dorfman LM, Adams GE* (1973) Nat Stand Ref Data Ser, Nat Bur Stand (U.S.A.), vol 46
[32] *Anbar M, Neta P* (1967) Int J Appl Radiat Isotopes 18: 493
[33] *Johnson GRA, Scholes G, Weiss J* (1953) J Chem Soc (London) 3091